



Clearance-induced vibration responses of mechanical systems: computational and experimental investigations

Selçuk Erkaya¹

Received: 8 September 2017 / Accepted: 6 November 2017 / Published online: 29 January 2018
© The Brazilian Society of Mechanical Sciences and Engineering 2018

Abstract

A suitable value of clearance in a joint connection is essential for the relative motion necessity of adjacent links. Even if the size of clearance is small, it should be considered at the governing equation of the system. During the mechanism motion, joint clearance is the basis of contact–impact forces between joint parts. In this study, clearance-induced dynamic responses of a spatial mechanism are investigated. Different clearance sizes and driving speeds are performed. For the computational approach, mechanism model is built using the simulation software ADAMS. The actual features of the system such as contact and friction are also considered at the model mechanism. A contact–impact model that comprises the impact function and the energy dissipation during the contact process is also utilized for the computational evaluations. At the experimental stage, clearance-induced vibrations are obtained from the system bearing as a reflection of impulsive forces. Two accelerometer sensors are used for necessary measurements. The results show that the clearance-based impulsive forces have crucial effects on the vibration responses. Clearance is a reason for the non-periodic vibration behaviors. Both the peak frequency and the vibration amplitude are affected from the clearance sizes and driving speeds.

Keywords Clearance-induced vibration · Contact–impact forces · Spatial mechanism · Spherical clearance joint · ADAMS · Multi-body dynamics

1 Introduction

A suitable value of clearance between the joint parts is essential for assemblage, relative mobility of neighbor links. This clearance leads to loss of kinematic constraints and the basis of unforeseeable contact–impact forces during the mechanism motion. These forces also worsen the dynamic responses of the system. Vibration is a result of improper system working, if the system's aim is not working based on the vibration theory. Vibration can cause not only decrease at the work quality but also acceleration at the wear, fatigue characteristics, etc. For these reasons, this topic has been frequently investigated by thematic researchers. In the last decades, clearance-induced

undesired effects such as vibration, noise, wear, fatigue have been studied.

Chen et al. [1] investigated the dynamics of a 2D slider–crank mechanism having clearance joint. The simulation software ADAMS with the impact function including the energy loss in the contact process was used for the computational approach. An experimental system was established to measure the accelerations for the case of different running speeds of mechanism. Farahan et al. [2] studied the nonlinear dynamic behavior of a four-bar mechanism having clearance joint between the coupler and rocker links. Contact–impact force model proposed by Lankarani–Nikravesh was utilized to evaluate the normal contact force developed on the contacting surface. Also, the friction effect between the clearance joint parts was modeled by using a modified Coulomb's friction law. Ebrahimi et al. [3] proposed a multiple scale method to perform the nonlinear vibrations of a mechanical system having dry or lubricated clearance joints. The Lankarani–Nikravesh model was used to describe the contact–impact force. Clearance size and lubricant viscosity were investigated to show the effects on frequency response and amplitude of

Technical Editor: Kátia Lucchesi Cavalca Dedini.

✉ Selçuk Erkaya
erkayaselcuk@gmail.com

¹ Mechatronics Engineering Department, Engineering Faculty, Erciyes University, 38039 Kayseri, Turkey

primary resonance. Ting et al. [4] presented an effective and simple kinematic methodology to define the position uncertainty arising from revolute or prismatic clearance joints for any linkage and manipulator. A numerical example based on three-leg planar 8-bar parallel robots was performed to verify the proposed approach. Zhu et al. [5] presented a comprehensive empirical investigation upon the wear calculation of a planar mechanism having clearance joint and discussed the empirical verification of nonlinear contact pressure distribution mode which was used to combine dynamic analysis including wear calculation. Khemili and Romdhane [6] investigated joint clearance effects on the dynamics of a planar slider–crank mechanism. An experimental test rig was also established to verify the obtained results. Flexibility of the mechanism link was investigated upon the compensation of clearance-induced problems. Ahmedalbashir et al. [7] proposed a spring addition to ensure the continuous contact relation between the parts of revolute clearance joint for improving the dynamic performance of a four-bar mechanism. Both theoretical studies of clearance-induced problems and their experimental verifications were performed for thematic researchers. Akhadkar et al. [8] investigated the effects of 3D revolute joints with radial and axial clearances on a circuit breaker mechanism. More contact points were studied in the numerical method. The numerical results were also validated by the experimental data. Erkaya et al. [9, 10] investigated the clearance effects on the kinematic and dynamic performance of the robotic and mechanical systems. Clearance-induced problems were modeled as optimization problems to decrease their undesired effects [11, 12]. Instead of classic joints, flexible connections between adjacent links were preferred to minimize the clearance based problems [13–15]. Noise and vibration behaviors of system having revolute clearance joint were also performed [16, 17]. Flexible link effects to compensate the clearance based problems were also studied [18, 19]. Artificial neural networks and fuzzy models were adapted to the open and closed loop multi-body systems for evaluating the system characteristics [20–22]. Flores et al. performed more studies about the clearance effects on multi-body dynamics. Theoretical and experimental investigations were performed by considering the planar and spatial mechanisms having clearance joint. Dry and viscous friction at the classic joint connection, different joint models (revolute, cylindrical and spherical joint types) and clearance values, different working conditions of mechanical system having rigid and flexible links were investigated [23–27]. Cammarata [28] proposed a novel method to find nodal displacements and rotations of over-constrained mechanisms due to clearance-affected joints. The virtual work principle was used for the proposed methodology. A spherical parallel manipulator was

considered for the theoretical investigation. The same model was also built and analyzed under the software ADAMS. Tian et al. [29] propose a new elastohydrodynamic lubricated spherical joint model for flexible multi-body dynamics. The proposed joint was also used to model the human gait artificial hip joints. Some numerical results were also verified using the commercial software ADINA. Wang et al. [30] investigated the dynamic model of a parallel mechanism with spherical clearance joint by considering the continuous contact between joint parts. Clearance joint was modeled as a no-mass rigid link. They also investigated the influence of the spherical joint clearance to predict the wear performance of spatial multi-body system [31]. Lankarani–Nikravesh contact force model and Archard’s wear model were preferred for dynamic equations. Same researchers investigated the effects of wear and flexibility on a five-bar mechanism with clearance joint [32]. The contact force model of Flores and co-workers was improved by the introduction of the stiffness coefficient. The Archard’s wear model was used to predict the wear depth. Tian et al. [33] presented a computational methodology to analyze the spatial flexible multi-body systems. The effects of the clearances and lubrication between the spherical joint parts were considered. The dry contact forces were evaluated based on a Hertzian contact law including the damping term dealing with the energy dissipation. The frictional forces were also performed using a modified Coulomb’s friction law. An investigation and comparison of several friction force models dealing with different friction phenomena in the context of multi-body system dynamics was presented by Marques et al. [34]. They also presented a new approach to model the spatial revolute joints having radial and axial clearances [35]. Newton–Euler approach was used for the new formulation based on the relative motion between the journal and bearing elements. Askari et al. [36] investigated the nonlinear vibration and dynamic behavior of a ceramic-on-ceramic hip implant. A spatial multi-body dynamic hip model was developed using a friction–velocity constitutive law combined with a Hertzian contact model. The friction-induced vibration on the contact point path was evaluated according to non-friction analysis. Zhang et al. [37] investigated the nonlinear stiffness of spherical joints. A new contact model for spherical joints based on the Winkler model and geometric constraints was established to calculate the stiffness of spherical joints with small clearances. Alves et al. [38] presented a comparative study on the most relevant existing viscoelastic contact force models. Hertz contact theory and energy dissipations during the impact process were considered in those models. The outcomes of the study were evaluated according to the selection of contact force model.

Clearance-induced contact–impact forces lead to unforeseeable vibration behaviors at the mechanical systems. Also, clearance characteristics have the deterministic role on the vibration responses. In this study, computational and experimental investigations are implemented to determine the exact outputs of clearance joint on the system performance. A spatial slider–crank mechanism is considered for having both the translational and the rotational motions. Different clearance sizes and driving speeds are studied together. Hertzian-based theory considering the Lankarani–Nikravesh model is preferred to evaluate the contact–impact forces between the ball and the socket parts. Also, the friction effects between the joint parts are modeled using the Coulomb’s friction law. For the computational investigation, a suitable model is built and analyzed using the simulation software ADAMS. A comparative evaluation with and without clearance joint are employed together how the non-ideal joint change the foreseeable vibration responses of multi-body systems. In the following steps, brief information about spherical clearance joint, contact force and the vibration equation of the system are given in Sect. 2. Simulation and experimental explanations are outlined in Sect. 3. Results and discussion are proposed in Sects. 4 and 5, respectively.

2 Modeling of spherical clearance joint, contact force and vibration equation

Clearance problem is unavoidable in articulated mechanisms because of the manufacturing, assemblage, wear phenomenon, etc. In fact, a suitable clearance value is essential to ensure the relative motion between the adjacent links. For a spherical joint, radial clearance is described as the difference between the radii of ball and socket parts of clearance joint. Also, the vector representation of clearance can be defined as the relative displacement of the ball center to the socket center. Due to the clearance between the ball and the socket parts, the most critical point is the loss of kinematic constraints. That is, the ideal kinematic pair at the mechanism connection disappears and two separate part relations in the joint become clear. Therefore, three possible motions can be observed as free-flight motion, impact and continuous contact modes. If the continuous contact motion is observed during the whole mechanism working, there is a similar character with ideal/perfect joint. However, this is so hard. During the mechanism motion, free-flight and the following impact motion modes also occur between the joint parts because of the motion necessity, inertial characters of links, etc. Particularly, these motion modes are bases of the deteriorations of kinematic and dynamic performances of mechanisms. Spherical clearance joint and contact force theories have

been outlined in the former studies. Readers can find the more textbook information about theoretical clarification in the thematic studies [23, 39]. Brief information is also given in this section. Therefore, Fig. 1 shows a spherical clearance joint representation in a mechanical system.

In Fig. 1, i th body is the socket part. Similarly, j th body denotes the ball part of spherical joint. \mathbf{e} is the clearance vector and this vector connects the socket and the ball centers as follows:

$$\mathbf{e} = \mathbf{r}_j^P - \mathbf{r}_i^P, \quad (1)$$

where both \mathbf{r}_i^P and \mathbf{r}_j^P are described in global coordinates with respect to the inertial reference frame [23, 39]. In the case of contact between the socket and the ball surfaces, relative penetration depth (δ) in Fig. 1b is described as

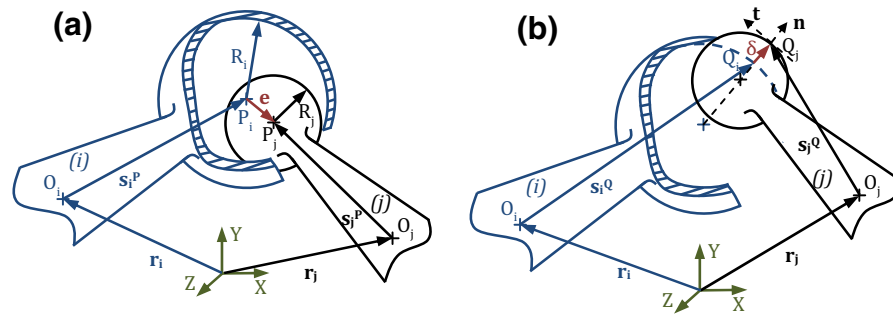
$$\delta = e - c. \quad (2)$$

In Eq. (2), e is the clearance vector magnitude, and c denotes the radial clearance which can be defined as the difference between the socket and the ball radii ($c = R_i - R_j$).

One of the most important and complex parts of the simulation of multi-body systems comprising the contact–impact analysis procedure is detection of the precise instant of impact. In addition, the used model to characterize the contact between the bodies requires the knowledge of the pre-impact conditions, that is, the impact velocity and the direction of the normal to the colliding surface. Neither the contact duration nor the penetration can be predicted from the pre-impact conditions due to the influence of the kinematic constraints and other interactions on the bodies of the complete system [40]. To evaluate efficiently the contact–impact forces resulting from collisions in multi-body systems, special attention must be given to the numerical description of the contact force model. Information on the impact velocity, material properties of the colliding bodies and geometry characteristics of the contact surfaces must be included into the contact force model [41]. Two different situations take place for the dynamics of a dry socket–ball. The first one is no contact force (\mathbf{F}_C) between the socket and the ball parts. In this situation, there is no any contact between the joint parts. This occurs due to the free motion of the ball part inside the socket part. The second one is the contact–impact forces due to the contact relation between the surfaces of the joint parts. These forces are modeled Hertzian-based contact theory (normal force, F_N) together with the Coulomb’s friction law (tangential force, F_T). These two conditions can be expressed as [23, 42, 43]

$$\mathbf{F}_C = \begin{cases} 0 & \text{if } \delta < 0 \\ F_N + F_T & \text{if } \delta \geq 0 \end{cases}, \quad (3)$$

Fig. 1 **a** Schematic illustration of a spherical clearance joint and **b** presentation of relative penetration between the joint parts [15, 23]



when the penetration depth is equal or greater than zero, an impact occurs and the contact force is modeled as a spring–damper element. If this element is linear, the approach is known as the Kelvin–Voigt model. When the relation is nonlinear, the model is generally based on the Hertz contact law [23, 44]. In the case of unlubricated joint, Hertzian contact force model is an appropriate choice [44]. While the original Hertzian model does not include any energy dissipation, an extension by Lankarani and Nikravesh includes energy loss due to internal damping. In a clearance joint, the contact force model is important to describe the collision dynamics between the ball and the socket parts [45, 46]. Due primarily to the simplicity of its contact force model, applicability to impact in multi-body systems, easy calculation and fast convergence (inclusion of energy dissipation modeling upon impact), the model developed by Lankarani and Nikravesh is widely used in dynamics of multi-body systems with joint clearance [41]. The effectiveness of the model proposed by Lankarani and Nikravesh was also proved by Flores et al. [47]. The normal force is expressed as [23, 24, 33, 43]

$$F_N = K\delta^{(3/2)} + D\dot{\delta}, \tag{4}$$

where the first component outlines the elastic force relation and the second term represents the energy dissipation. D is the coefficient of hysteresis damping. K is the generalized stiffness parameter [23, 24, 33, 43]

$$K = \frac{4(E_i E_j)}{3(E_j(1 - \nu_i^2) + E_i(1 - \nu_j^2))} \left(\frac{R_i R_j}{R_i - R_j} \right)^{1/2}. \tag{5}$$

The stiffness parameter depends on the material properties and the shape of the contact surfaces. For this reason, in Eq. (5), ν and E are the Poisson’s ratio and the Young’s modulus for each body at the contacting point. The coefficient of hysteresis damping is defined as [43]

$$D = \frac{3(1 - \zeta^2)K\delta^{(3/2)}}{4v_0}, \tag{6}$$

where ζ is the restitution coefficient and v_0 is the initial impact velocity. In the simulation software, the normal force function is calculated by [48]

$$F_N = \begin{cases} K\delta^{(3/2)} + \text{STEP}(\delta, 0, 0, d_{\max}, C_{\max}) \frac{d\delta}{dt} & \text{for } \delta \geq 0 \\ 0 & \text{for } \delta < 0 \end{cases}. \tag{7}$$

In Eq. (7), the coefficient of hysteresis damping is also calculated by

$$\text{STEP}(\delta, 0, 0, d_{\max}, C_{\max}) = \begin{cases} 0 & \text{for } \delta \leq 0 \\ C_{\max}(\delta/d_{\max})^2(3 - 2(\delta/d_{\max})) & \text{for } 0 < \delta < d_{\max} \\ C_{\max} & \text{for } \delta \geq d_{\max} \end{cases}, \tag{8}$$

where d_{\max} is a positive real value for the boundary penetration. C_{\max} is the coefficient of maximum damping. When contacting, bodies slide or tend to slide relative to each other. There are forces generated which are tangential to the surfaces of contact. These forces are usually referred to as friction forces. Friction is a complex phenomenon due to many physical and working parameters [49]. It can be seen in all multi-body systems. It includes the interaction between the contacting surfaces and may cause to different friction regimes (sliding and sticking) [34]. In general, Coulomb’s friction model is preferred to represent the friction response in impact and contact process. However, the definition of the Coulomb’s friction law poses numerical difficulties when the relative tangential velocity is in the vicinity of zero. In the current study, the following model is used to represent the friction behavior between the joint parts [50].

$$F_T = -\mu(v_T)F_N \frac{\mathbf{v}_T}{|v_T|}, \tag{9}$$

where $\mu(v_T)$ is the coefficient of dynamic friction and is not a constant value. It is introduced in the used Coulomb friction model. $\mu(v_T)$ is a function of tangential sliding

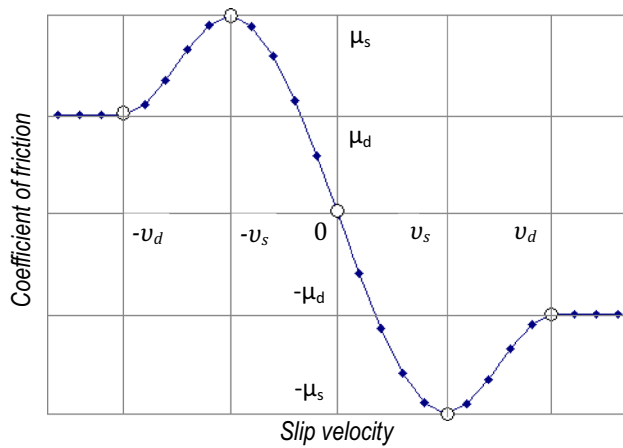


Fig. 2 Coefficient of friction varying with slip velocity [14, 48, 50]

velocity in collision plane, which can represent the friction behavior in impact and contact process as well as the viscous and micro-slip phenomenon in relative low-velocity case more accurately. And also, the selected Coulomb’s friction model can avoid the case of abrupt change of friction in numerical calculation as the change of velocity

direction [43, 50]. The coefficient of dynamic friction in simulation software is calculated by

$$\mu(v_T) = \begin{cases} -\mu_d \text{sign}(v_T) & \text{for } |v_T| > v_d \\ -\text{STEP}(|v_T|, v_d, \mu_d, v_s, \mu_s) \text{sign}(v_T) & \text{for } v_s \leq |v_T| \leq v_d \\ \text{STEP}(v_T, -v_s, \mu_s, v_s, -\mu_s) & \text{for } |v_T| < v_s \end{cases} \quad (10)$$

In Eq. (10), μ_s and μ_d are the coefficients of static and dynamic frictions, respectively. v_s and v_d denote the critical velocities of static and maximum dynamic frictions, respectively. Figure 2 outlines the relation between the dynamic friction coefficient and slip velocity.

By considering the Newtonian dynamics, the general mathematical model of the vibration is simply written as [51],

$$M_S \ddot{\mathbf{q}}(t) + C_S \dot{\mathbf{q}}(t) + K_S \mathbf{q}(t) = \mathbf{F}_G(t) + \mathbf{F}_C(\delta, \dot{\delta}), \quad (11)$$

where M_S , C_S and K_S are the mass, damping and stiffness of system, respectively. \mathbf{q} denotes the generalized coordinates. $\dot{\mathbf{q}}$ and $\ddot{\mathbf{q}}$ are the first- and second-order time derivatives of generalized coordinates, respectively. \mathbf{F}_G denotes the general force and is usually periodic character. In the

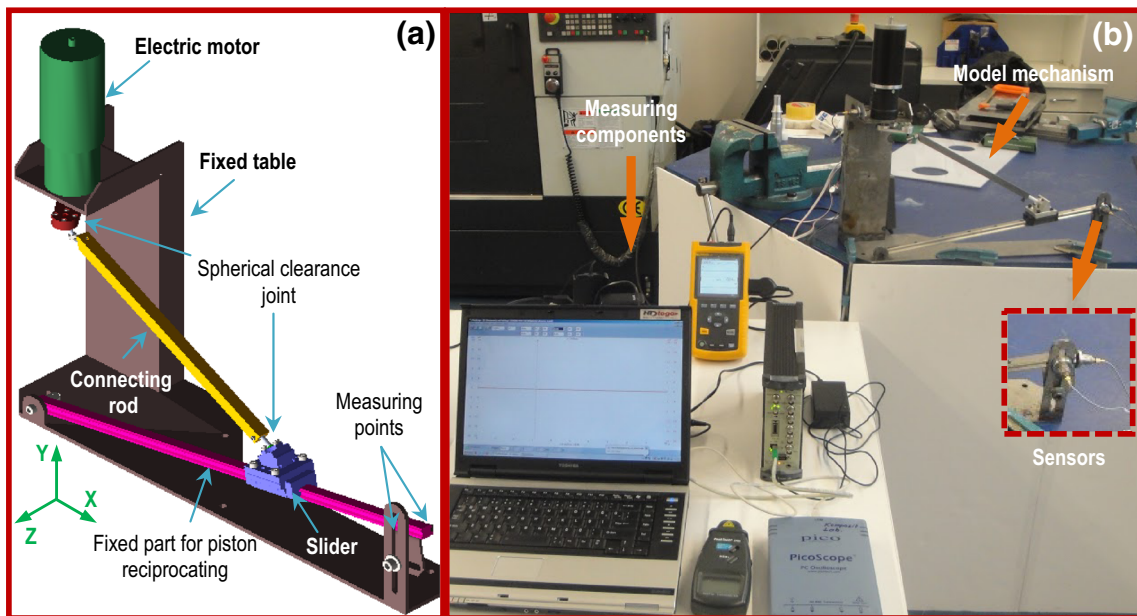


Fig. 3 Model mechanism: a simulation model and b experimental model

Table 1 Geometric, mass and inertia characters of model mechanism

Links	Length (mm)	Mass (kg)	Mass moment of inertia characteristics (kg mm ²)		
			I_{xx}	I_{yy}	I_{zz}
Crank	50	0.104	6.64	57.11	52.51
Connecting rod	329	0.455	15.31	3489.75	3490.43
Slider	–	0.553	148.12	225.14	209.02

Table 2 Used parameters in the dynamic simulation

Description	Value
Coefficient of friction	0.03
Coefficient of restitution	0.90
Poisson's coefficient	0.3
Young's modulus	207 GPa
Integrator scheme	Gear
Integration step size	1×10^{-3} s
Integration tolerance	1×10^{-5}

case of clearance joint connection, F_C is the contact-impact force produced by clearance joint parts during the

working of system. This force takes place during a small time interval at the termination of the free-flight motion. It has a non-periodic form and fully affects the system dynamics. It is mainly basis of the unforeseeable vibration responses of the system.

3 Simulation and experimental models

Due to having both the translational and the rotational motions, a spatial slider-crank mechanism was considered in the current investigation. At the computational approach, mechanism model was built under the software ADAMS to evaluate the contact-impact forces on the slider bearing. For the experimental stage, full system was established to

Fig. 4 Spherical joints having clearances, **a** 0.25 mm clearance size and **b** 0.5 mm clearance size

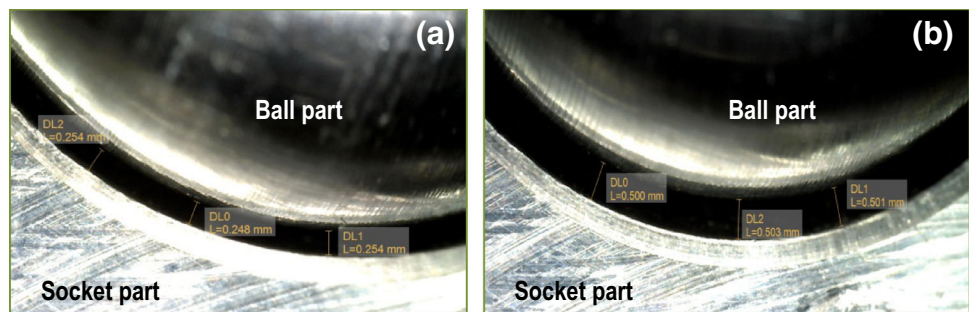
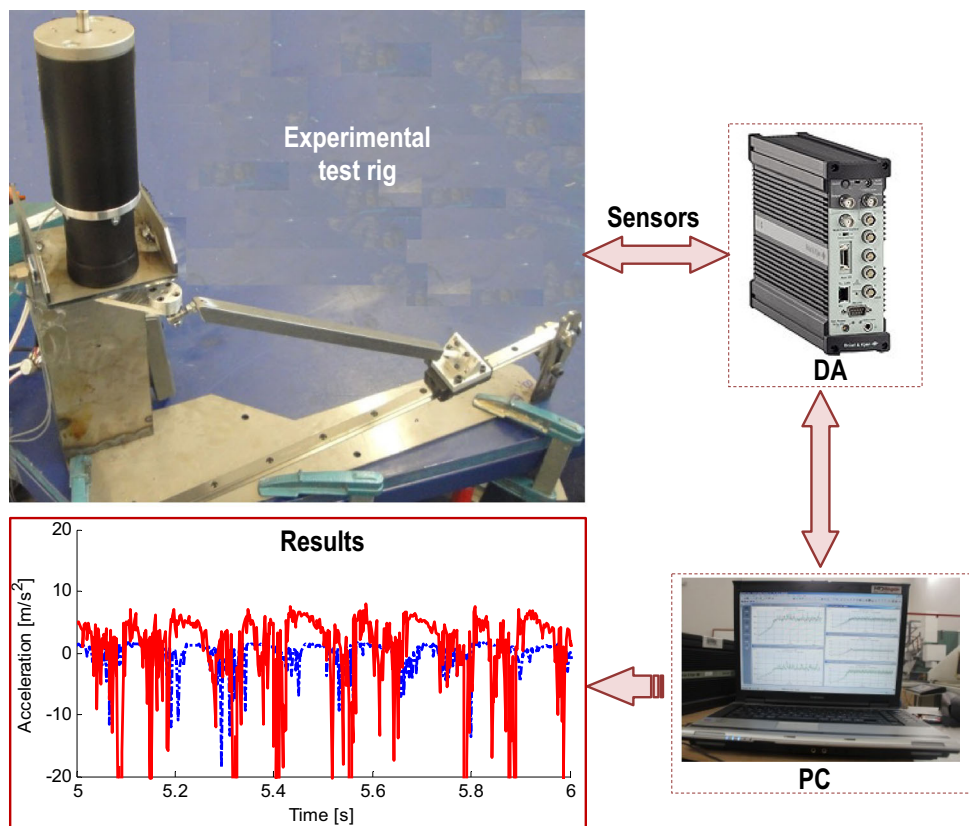


Fig. 5 Schematic diagram of experimental measurement [13, 15]



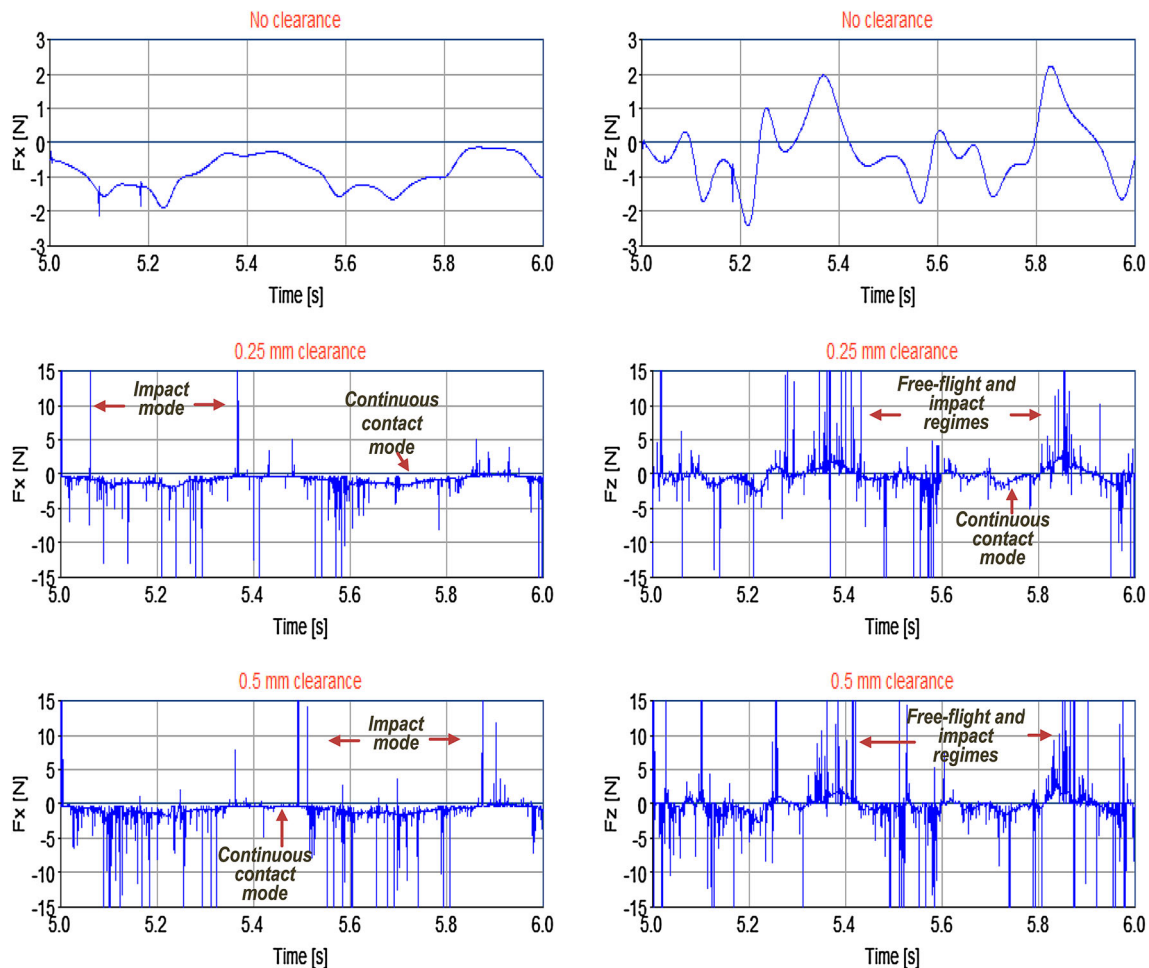


Fig. 6 Slider-fixed bearing force components for 125 rpm crank speed

analyze the clearance-induced vibration response on the bearing. The schematic presentation of model mechanism is outlined in Fig. 3.

The crank link was connected by an electric motor to actuate the system as 125 and 250 rpm running speeds. A speed control unit and a digital tachometer were used for controlling and verifying the input link's rotational speed. The geometric and mass characters of the model mechanism are outlined in Table 1.

Dynamic simulation parameters are outlined in Table 2.

Model mechanism has two spherical joints among the crank, connecting rod and slider links. The diameters of the ball and the socket parts are arranged to ensure the 0.25 and 0.5 mm artificial clearance values. Owing to the different motion modes between the joint parts, clearance-induced vibration responses were obtained from two different points to measure the reflections of the contact-impact forces during the mechanism working. To evaluate the exact contribution of clearance joint, the vibration characteristics arising from only actuator and its components are first measured without any assemblage to the

mechanism. The mean value of this measurement is separated from the vibration of full system working. Also, clearance joint parts were cleaned by alcohol to remove the manufacturing residuals before the experimental studies. Two accelerometer sensors were positioned at the slider bearing (Fig. 3b). Brüel and Kjaer data acquisition (DA) and accelerometer sensors were employed for the experimental measurements [14, 16]. The total mass of each sensor and magnet is 25×10^{-3} kg. A digital camera having $41 \times$ zoom was used for showing the real clearance values between spherical joint parts. Figure 4 gives the differences between the ball and the socket diameters.

The socket part was manufactured as two symmetric parts to ensure the easy assemblage of different ball parts. The schematic diagram for experimental measurement is represented in Fig. 5.

In the stage of experimental measurement, same test rig was used for model mechanisms with and without clearance joint. As measuring components, a data acquisition, two accelerometer sensors at the slider-fixed bearing and a computer were used to evaluate the vibration responses of

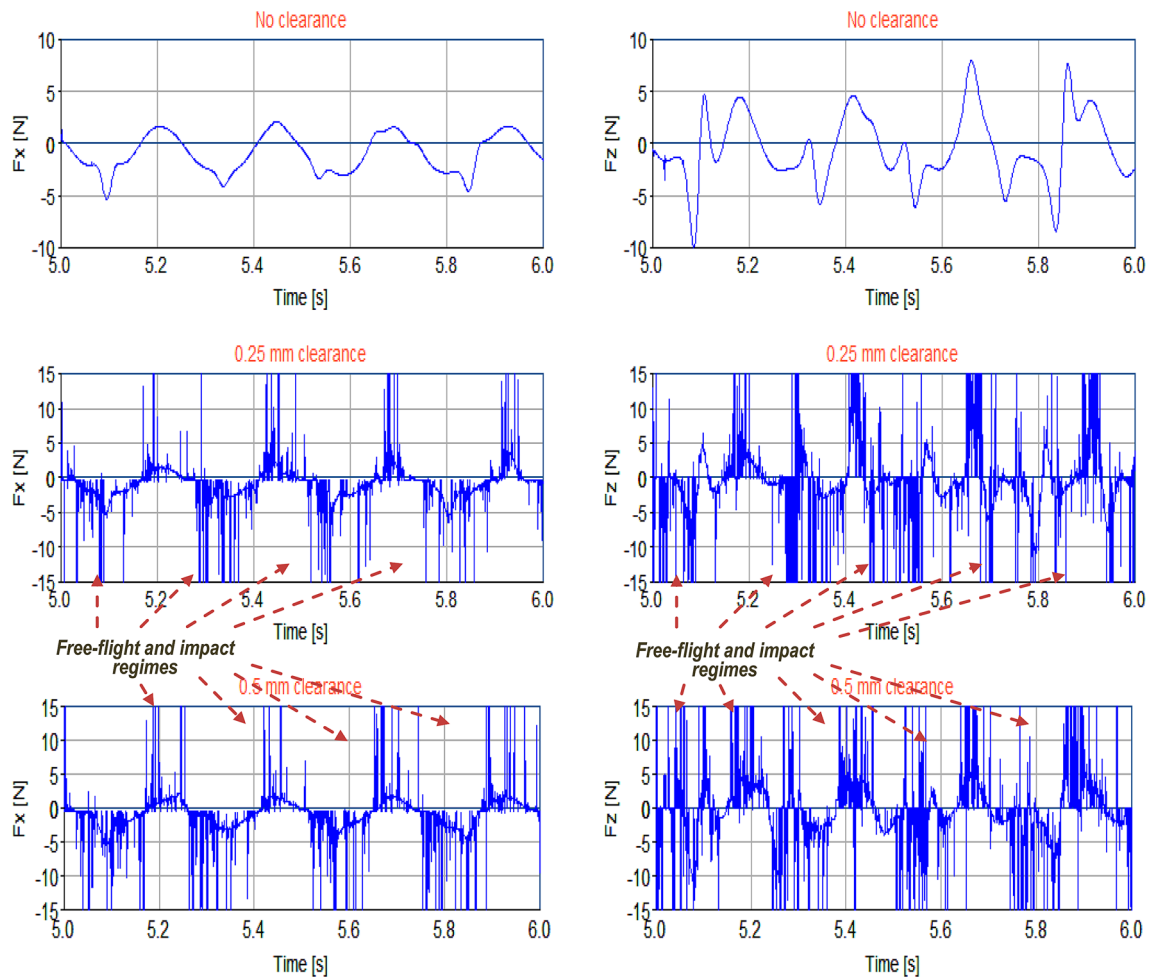


Fig. 7 Slider-fixed bearing force components for 250 rpm crank speed

model mechanisms. The sampling frequency of vibration measurement was arranged as 500 Hz. For the starting position of mechanisms models, that is, the connecting rod and fixed part for piston reciprocating were arranged at the same plane (XY plane). The vibration data was collected for the case of different driving speeds and clearance sizes. While the mechanisms reached the stable driving speeds, the parts of these data were used for exact evaluations.

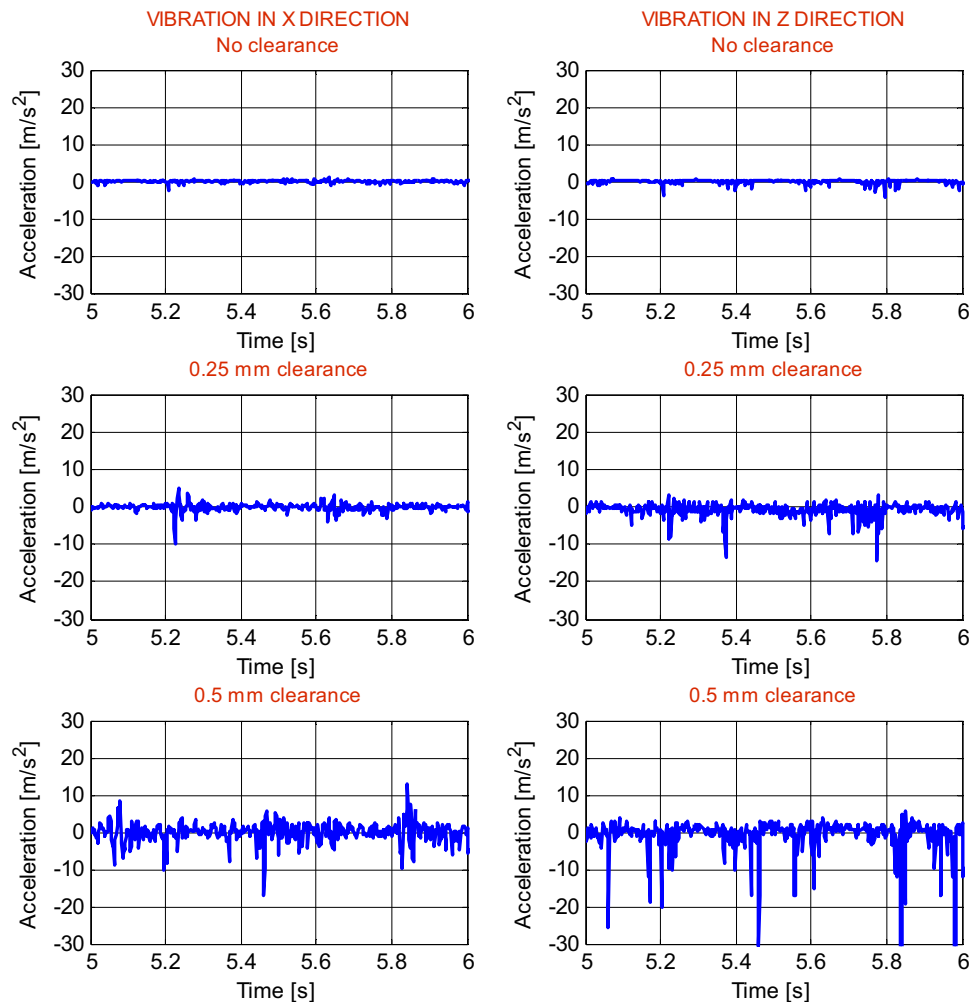
4 Results

In the current study, the computational and experimental stages were performed for investigating the clearance-induced impulsive forces and vibration responses of a spatial multi-body system. A slider–crank mechanism was considered for case studies. Spherical clearance joints were used among the crank, connecting rod and slider links. For ensuring the different clearance sizes in spherical joints, the diameter of socket part was manufactured as 12 mm. At the same time, the diameters of ball parts were

manufactured as 11 and 11.5 mm. Therefore, clearance values were arranged as 0.25 and 0.5 mm between joint parts. 125 and 250 rpm driving speeds were applied to the crank link. The software ADAMS was used for the computational analyzing. In addition, an experimental study was performed to measure the vibration responses. To evaluate the exact reflection of joint clearance, vibrations arising from only electric motor and its assemblage apparatus were measured without any assemblage to the model mechanisms. After measuring the whole system vibration, the mean vibration value of electric motor and its assemblage apparatus was separated from the whole system vibration response. For the computational study, simulations were performed in an Intel Xeon computer. It is clear from the simulations that much more computation time, nearly upwards of ten times, is necessary in the case of mechanism with clearance joint [9, 13, 52]. Bearing forces for case studies are outlined in Figs. 6 and 7.

In the case of mechanism having clearance joint, the values of force components are beyond the given figure scale. For clarity and easy comparison, figure scales are

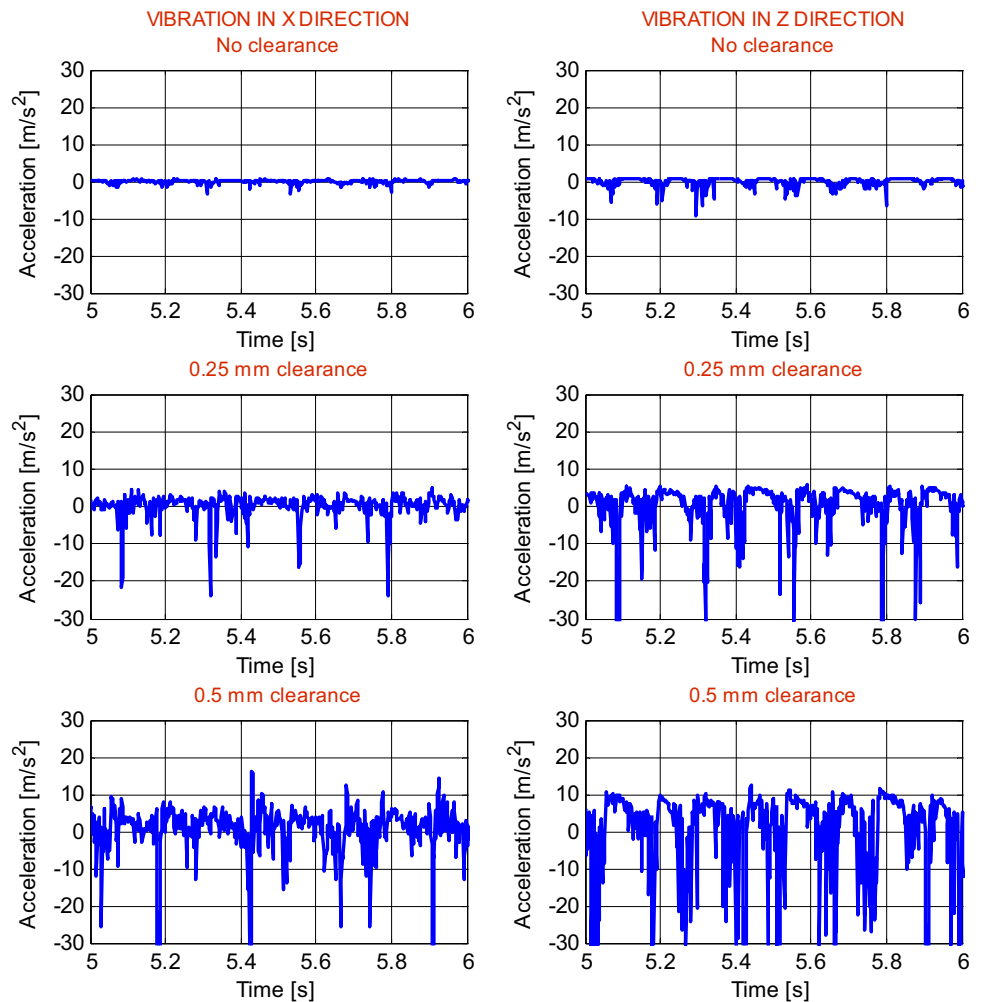
Fig. 8 Vibration response of slider-fixed bearing for 125 rpm crank speed



limited as possible as. As seen from the figures, there are clear differences for bearing forces of mechanisms with and without clearances [6, 24]. Due to the clearance, there are some peaks at the force components. At the higher driving speed, the sequential peaks, that is, contact-impact forces are seen extensively. Also, even if the driving speed is same, the higher size of clearance value is the dominant factor for these extensive peaks. These forces' peaks take place during a small time interval [13–15, 24]. These impulsive forces lead to non-periodic input characters for the vibration behavior of the system. Both clearance value and driving speed affect these peak characters [18]. The higher driving speed leads to increases in peak frequency. Force peak frequency is directly dealing with the contact-impact phenomenon between the clearance joint parts. More peaks mean that more contact-impact forces. Also, the bigger values of clearance sizes have a crucial effect on the force amplitude [10, 18]. The experimental results for the vibration responses of the mechanisms with and without clearance are outlined in Figs. 8 and 9.

As seen from the figures, while the vibration response of mechanism without clearance is naturally periodic, the mechanism having clearance joint has an aperiodic vibration behavior. That is a reason of contact-impact force effects. These forces that are produced for a small time interval change the foreseeable vibration results. Clearance values and/or driving speed have crucial effects on the vibration responses [14, 16]. Both the peak frequency and the vibration amplitude increase at the mechanism having clearance joint. Higher values of clearance size and driving speed have dominant effects on the higher peak frequency and amplitude of bearing vibration. These make the whole system performance worse [6]. Wear, fatigue, expected work quality, etc., decrease due to the clearance joint. From the evaluation of all figures, both force and naturally vibration responses are bigger in z direction. This arises from the oscillation of connecting rod link during the mechanism motion.

Fig. 9 Vibration response of slider-fixed bearing for 250 rpm crank speed



5 Conclusion

Both computational and experimental studies of a 3D slider-crank mechanism with and without clearance joints are investigated. Different clearance sizes and driving speeds are considered for case studies. Clearance is inevitable between the movable joint parts for relative motion necessity of neighbor links. Different motion modes between the joint parts and the vibration results of these modes are evaluated together. As seen from the results, the impulsive forces have crucial effects on the system dynamics. These forces occur for a small time interval and they are observed at the termination of the free-flight mode between joint parts. Non-periodic characters are seen for force and vibration responses. Even if the clearance size is small, it should be considered for the exact analysis due to the loss of kinematic constraints at the joint connection. Unforeseeable responses of clearance joints decrease the system performance. Peak frequency and vibration amplitude have significant relations with clearance size and driving speed. Obtained results and evaluations should be considered for

performing the vibration control strategy and selecting the optimum vibration isolator. In the current study, the dry contact between joint parts is considered. In the case of lubrication between joint parts, the clearance-induced vibration may be reduced due to the viscous damping character of lubrication. Also, this may be a better solution for thermal problems of metal-to-metal contact between joint parts. This is an ongoing study. In the following steps, wear and fatigue characters of the system, lubrication and thermal effects between the joint parts, active and/or passive controller design will be studied for the clearance-induced problems.

References

1. Chen Y, Sun Y, Yang D (2017) Investigations on the dynamic characteristics of a planar slider-crank mechanism for a high-speed press system that considers joint clearance. *J Mech Sci Technol* 31(1):75–85

2. Farahan SB, Ghazavi MR, Rahmanian S (2017) Bifurcation in a planar four-bar mechanism with revolute clearance joint. *Nonlinear Dyn* 87(2):955–973
3. Ebrahimi S, Salahshoor E, Maasoomi M (2017) Application of the method of multiple scales for nonlinear vibration analysis of mechanical systems with dry and lubricated clearance joints. *J Theor Appl Vib Acoust* 3(1):41–60
4. Ting KW, Hsu KL, Wang J (2017) Clearance-induced position uncertainty of linkages and parallel manipulators. *J Mech Robot* 9(6):061001
5. Zhu A, He S, Zhao J, Luo W (2017) A nonlinear contact pressure distribution model for wear calculation of planar revolute joint with clearance. *Nonlinear Dyn* 88(1):315–328
6. Khemili I, Romdhane L (2008) Dynamic analysis of a flexible slider–crank mechanism with clearance. *Eur J Mech A Solids* 27:882–898
7. Ahmedalbashir M, Romdhane L, Lee J (2017) Dynamics of a four-bar mechanism with clearance and springs—modeling and experimental analysis. *J Mech Sci Technol* 31(3):1023–1033
8. Akhadkar N, Acary V, Brogliato B (2017) Multibody systems with 3D revolute joints with clearances: an industrial case study with an experimental validation. *Multibody Syst Dyn*. <https://doi.org/10.1007/s11044-017-9584-5>
9. Erkaya S (2012) Investigation of joint clearance effects on welding robot manipulators. *Robot Comput Integr Manuf* 28:449–457
10. Erkaya S, Uzmay İ (2009) Investigation on effect of joint clearance on dynamics of four-bar mechanism. *Nonlinear Dyn* 58:179–198
11. Erkaya S, Uzmay İ (2009) Determining link parameters using genetic algorithm in mechanisms with joint clearance. *Mech Mach Theory* 44:222–234
12. Erkaya S, Uzmay İ (2009) Optimization of transmission angle for slider–crank mechanism with joint clearances. *Struct Multidiscipl Optim* 37:493–508
13. Erkaya S, Doğan S (2015) A comparative analysis of joint clearance effects on articulated and partly compliant mechanisms. *Nonlinear Dyn* 81:323–341
14. Erkaya S, Doğan S, Ulus Ş (2015) Effects of joint clearance on the dynamics of a partly compliant mechanism: numerical and experimental studies. *Mech Mach Theory* 88:125–140
15. Erkaya S, Doğan S, Şefkatlioğlu E (2016) Analysis of the joint clearance effects on a compliant spatial mechanism. *Mech Mach Theory* 104:255–273
16. Erkaya S, Uzmay İ (2010) Experimental investigation of joint clearance effects on the dynamics of a slider–crank mechanism. *Multibody Syst Dyn* 24:81–102
17. Erkaya S (2012) Prediction of vibration characteristics of a planar mechanism having imperfect joints using neural network. *J Mech Sci Technol* 26:1419–1430
18. Erkaya S, Uzmay İ (2014) Modeling and simulation of joint clearance effects on mechanisms having rigid and flexible links. *J Mech Sci Technol* 28:2979–2986
19. Erkaya S (2012) Effects of balancing and link flexibility on dynamics of a planar mechanism having joint clearance. *Sci Iran* 19:483–490
20. Erkaya S (2013) Trajectory optimization of a walking mechanism having revolute joints with clearance using ANFIS approach. *Nonlinear Dyn* 71:75–91
21. Erkaya S, Uzmay I (2008) A neural–genetic (NN–GA) approach for optimising mechanisms having joints with clearance. *Multibody Syst Dyn* 20:69–83
22. Erkaya S (2017) Effects of joint clearance on motion accuracy of robotic manipulators. *J Mech Eng*. <https://doi.org/10.5545/sv-jme.2017.4534>
23. Flores P, Ambrósio J, Claro JC, Lankarani HM (2006) Dynamics of multibody systems with spherical clearance joints. *J Comput Nonlinear Dyn* 1:240–247
24. Flores P, Koshy C, Lankarani H, Ambrósio J, Claro JCP (2011) Numerical and experimental investigation on multibody systems with revolute clearance joints. *Nonlinear Dyn* 65:383–398
25. Tian Q, Liu C, Machado M, Flores P (2011) A new model for dry and lubricated cylindrical joints with clearance in spatial flexible multibody systems. *Nonlinear Dyn* 64:25–47
26. Flores P, Lankarani HM (2010) Spatial rigid-multibody systems with lubricated spherical clearance joints: modeling and simulation. *Nonlinear Dyn* 60:99–114
27. Flores P, Ambrósio J, Claro JCP, Lankarani H (2006) Spatial revolute joints with clearances for dynamic analysis of multibody systems. *Proc Inst Mech Eng Part K J Multibody Dyn* 220:257–271
28. Cammarata A (2017) A novel method to determine position and orientation errors in clearance-affected overconstrained mechanisms. *Mech Mach Theory* 118:247–264
29. Tian Q, Lou J, Mikkola A (2017) A new elastohydrodynamic lubricated spherical joint model for rigid-flexible multibody dynamics. *Mech Mach Theory* 107:210–228
30. Wang G, Liu H, Deng P (2014) Dynamic modeling for a parallel mechanism considering spherical joint clearance. *J Vib Shock* 10:009
31. Wang G, Liu H, Deng P (2015) Dynamics analysis of spatial multibody system with spherical joint wear. *J Tribol* 137(2):021605
32. Wang G, Liu H (2017) Dynamic analysis and wear prediction of planar five-bar mechanism considering multiflexible links and multiclearance joints. *J Tribol* 139(5):051606
33. Tian Q, Zhang Y, Chen L, Flores P (2009) Dynamics of spatial flexible multibody systems with clearance and lubricated spherical joints. *Compos Struct* 87:913–929
34. Marques F, Flores P, Claro JCP, Lankarani HM (2016) A survey and comparison of several friction force models for dynamic analysis of multibody mechanical systems. *Nonlinear Dyn* 86(3):1407–1443
35. Marques F, Isaac F, Dourado N, Flores P (2017) An enhanced formulation to model spatial revolute joints with radial and axial clearances. *Mech Mach Theory* 116:123–144
36. Askari E, Flores P, Dabirrahmani D, Appleyard R (2014) Nonlinear vibration and dynamics of ceramic on ceramic artificial hip joints: a spatial multibody modelling. *Nonlinear Dyn* 76(2):1365–1377
37. Zhang J, Guo HW, Liu RQ, Deng ZQ (2015) Nonlinear characteristic of spherical joints with clearance. *J Aerosp Technol Manag* 7(2):179–184
38. Alves J, Peixinho N, Silva MT, Flores P, Lankarani HM (2015) A comparative study of the viscoelastic constitutive models for frictionless contact interfaces in solids. *Mech Mach Theory* 85:172–188
39. Askari E, Flores P, Dabirrahmani D, Appleyard R (2015) Dynamic modeling and analysis of wear in spatial hard-on-hard couple hip replacements using multibody systems methodologies. *Nonlinear Dyn* 82:1039–1058
40. Flores P, Ambrósio J (2010) On the contact detection for contact–impact analysis in multibody systems. *Multibody Syst Dyn* 24:103–122
41. Lankarani H, Nikravesh P (1990) A contact force model with hysteresis damping for impact analysis of multibody systems. *J Mech Des* 112:369–376
42. Zheng E, Zhu R, Zhu S, Lu X (2016) A study on dynamics of flexible multi-link mechanism including joints with clearance and lubrication for ultra-precision presses. *Nonlinear Dyn* 83:137–159

43. Flores P, Ambrósio J, Claro JCP, Lankarani H, Koshy C (2006) A study on dynamics of mechanical systems including joints with clearance and lubrication. *Mech Mach Theory* 41:247–261
44. Ravn P (1998) A continuous analysis method for planar multibody systems with joint clearance. *Multibody Sys Dyn* 2:1–24
45. Flores P, Machado M, Silva MT, Martins JM (2011) On the continuous contact force models for soft materials in multibody dynamics. *Multibody Syst Dyn* 25:357–375
46. Machado M, Moreira P, Flores P, Lankarani HM (2012) Compliant contact force models in multibody dynamics: evolution of the Hertz contact theory. *Mech Mach Theory* 53:99–121
47. Flores P, Ambrósio J, Claro JP, Lankarani HM (2008) Kinematics and dynamics of multibody systems with imperfect joints: models and case studies. Springer, Berlin
48. MSC ADAMS (2013) Automatic dynamic analysis of mechanical systems. MSC Software Corporation, Santa Ana
49. Pennestri E, Rossi V, Salvini P, Valentini PP (2016) Review and comparison of dry friction force models. *Nonlinear Dyn* 83:1785–1801
50. Bai ZF, Zhao Y (2013) A hybrid contact force model of revolute joint with clearance for planar mechanical systems. *Int J Non-Linear Mech* 48:15–36
51. Rao SS (1990) Mechanical vibrations, 2nd edn. Addison-Wesley, USA
52. Flores P (2010) A parametric study on the dynamic response of planar multibody systems with multiple clearance joints. *Nonlinear Dyn* 61:633–653